Agricultural and Forest Meteorology 259 (2018) 355–363

Contents lists available at ScienceDirect

Agricultural and Forest Meteorology

journal homepage: www.elsevier.com/locate/agrformet

# Partitioning evapotranspiration using an optimized satellite-based ET model across biomes

Chunjie Gu[a], Jinzhu Ma[a,*], Gaofeng Zhu[a], Huan Yang[a], Kun Zhang[a], Yunquan Wang[b], Chunli Gu[c]

[a] Key Laboratory of Western China's Environmental Systems (Ministry of Education), College of Earth and Environmental Sciences, Lanzhou University, 222 South Tianshui Road, Lanzhou, 730000, China
[b] School of Environmental Studies, China University of Geosciences at Wuhan, 430074, China
[c] Beijing Institute of Applied Meteorology, Beijing, 100029, China

ARTICLE INFO

*Keywords:*
Evapotranspiration partition
Biomes
Satellite-based ET model
Canopy interception evaporation
Transpiration ratio

ABSTRACT

The partitioning of evapotranspiration (ET) is a critical factor in the terrestrial water balance and global water cycle, and understanding the partitioning across terrestrial biomes and the relationships between ET partitions and potential influencing factors is critical for predicting future ecosystem feedbacks. Based on an optimized Priestly-Taylor Jet Propulsion Laboratory model, we partitioned ET into three components transpiration (T), canopy interception evaporation (EI), and soil evaporation (ES). We found the components of EI to be significant with the ratio of EI to precipitation ranging from 0.02 to 0.29 across different biomes. The T/ET ratio ranged from 0.29 to 0.72 with obvious differences across biomes and with ratios generally lower than in previous studies with isotope-based methods. The (T + EI)/ET ratio was limited to a relatively narrow band from 0.57 to 0.86. The T/ET values show an obvious decreasing trend with increasing annual precipitation, but there was no significant correlation between T/ET and annual leaf area index.

## 1. Introduction

Evapotranspiration (ET) is a pivotal process for ecosystem water budgets and accounts for a substantial portion of the global energy balance (Seneviratne et al., 2006; Trenberth et al., 2009; Liu et al., 2016). ET has three components: transpiration (T), canopy interception evaporation (EI), and soil evaporation (ES). Transpiration is a biological process closely linked to ecosystem productivity, while EI and ES are physical processes representing evaporation from wet canopy surfaces or soil (Scott et al., 2006). The components of ET may affect long-term plant evolution and groundwater stores (Miralles et al., 2011). Accounting for the ET components across different biomes is essential for the evaluation of the impacts of carbon dioxide enrichment and land use changes (Sutanto et al., 2012; Schlesinger and Jasechko, 2014; Fisher et al., 2017). Recently, more attention has been given to the quantification of the different components of ET in the global water cycle (Maxwell and Condon, 2016; Wei et al.,2017); however, the results obtained by the various methods show obvious differences and a unified consensus on the best methodology has not been achieved.

Three general categories of techniques have been used to quantify the components of ET. A combination of hydrometric methods, such as lysimeters, sap flow, Bowen ratio techniques, or eddy covariance (a type of direct measurement of transpiration), have been used for this purpose for several decades (Herbst et al., 1996; Ffolliott et al., 2003; Barbour et al., 2005; Roupsard et al., 2006; Mitchell et al., 2009; Cavanaugh et al., 2011; Raz-Yaseef et al., 2012). Isotope-based methods, using the ratios of oxygen ($^{18}O/^{16}O$) and hydrogen ($^{2}H/^{1}H$), have been used to separate ET components because evaporation and transpiration have different isotopic fractionation on the stable isotope ratios in water (Yakir and Wang, 1996; Yepez et al., 2003; Ferretti et al., 2003; Xu et al., 2008; Rothfuss et al., 2010; Wang et al., 2012; Jasechko et al., 2013). Finally, land-surface models, using climatological and vegetation parameters, combine the water balance method with ET models to estimate large-scale ET partitions (Choudhury and DiGirolamo, 1998; Dirmeyer et al., 2006; Lawrence et al., 2007; Miralles et al., 2011; Blyth and Harding, 2011; Maxwell and Condon, 2016; Wei et al., 2017; Fatichi and Pappas, 2017). Each type of technique has advantages and limitations. Hydrometric measurements and isotope-based methods are restricted by experimental costs and the required observation period; many studies have focused only on one period or growing season which can be misleading. Models can overcome this, but the reliability of modeling simulations is decreased because of the substantial number of parameters.

Research on the T/ET ratio has attracted much attention. Using the

* Corresponding author.
*E-mail address:* jzma@lzu.edu.cn (J. Ma).

https://doi.org/10.1016/j.agrformet.2018.05.023
Received 12 July 2017; Received in revised form 21 May 2018; Accepted 28 May 2018
Available online 02 June 2018
0168-1923/ 

isotope mass balance method, Jasechko et al. (2013) noted that transpiration could account for nearly 80–90% of the total ET from continents. However, using the same method with a different set of input data, Coenders-Gerrits et al. (2014) showed the transpiration portion of ET to be lower, at 35–80%. Kool et al. (2014) reviewed 52 studies to compare different approaches for partitioning ET and found that transpiration was less than 70% of ET in 32 of the studies. Schlesinger and Jasechko (2014) compiled 81 studies that partitioned ET into transpiration and evaporation (ignoring canopy interception) with results that indicated that transpiration accounted for 61% ( ± 15%) of ET. Using about 23ET partitioning studies, Sutanto et al. (2014) gave a perspective on isotope-based versus non-isotope-based approaches and found that numerous isotope-based studies reported transpiration to be generally more than 70% of ET, hydrometric methods reported transpiration fractions exceeding 50% on average, and global land-surface models produced lower fractions (approximately 50%). Maxwell and Condon (2016) utilized a continental-scale hydrologic model to study the influence of lateral ground water flow on ET partitioning and found transpiration fractions of ET ranging from 47 ± 13% to 62 ± 12% after adding lateral groundwater flow. The fraction of T/ET from previous studies indicates large variability caused by great uncertainty of estimation, suggesting that obtaining a high accuracy for the ratio remains a challenging issue. Furthermore, there were fewer research studies that focus on the diversity of ET segmentation across different biomes and potential influencing factors in previous studies (Schlesinger and Jasechko, 2014; Wei et al., 2017).

The interception evaporation (EI) of vegetation, a significant part of ET, can exert a strong influence on continental water resources (Muzylo et al., 2009; Miralles et al., 2010, 2011). Llorens and Domingo (2007) reviewed experimental studies under Mediterranean conditions and found the ratio of average interception rate to precipitation for trees and shrubs. Miralles et al. (2010) obtained canopy interception from satellite observations over broadleaf evergreen forests, broadleaf deciduous forests, and needleleaf forests. The following year they used the GLEAM model to derive the different components of daily actual ET globally. Other studies have forced the comparison of results with different segmentation methods, but have encountered difficulties distinguishing and determining the influencing factors of various biomes.

With the development of remote sensing technology, many researchers have used ET models derived from satellite observations (Choudhury and DiGirolamo, 1998; Cleugh et al., 2007; Mu et al., 2007, 2011; Fisher et al., 2008; Zhang et al., 2010; Liu et al., 2016). Among these models, the Priestly-Taylor Jet Propulsion Laboratory (PT-JPL) model proposed by Fisher et al. (2008) has provided the best results across multiple flux towers (Ershadi et al., 2014; Feng et al., 2015; Zhu et al., 2016; McCabe et al., 2016). For the PT-JPL model combines relatively few ecophysiological parameters, Zhang et al. (2017) used the parameter sensitivity analysis method to identify three most sensitive parameters, and obtained better simulation results with the Bayesian approach of the differential evolution Markov chain (DE-MC) algorithm to optimize the PT-JPL model.

Based on the long-term observed data from FLUXNET across different biomes, the PT-JPL model could provide an operational opportunity for estimating the different components (i.e. T, EI and ES) in total ET. Here, drawing on the approach of sensitive parameters optimization from Zhang et al. (2017), we obtain the partition results of ET. In this context, we address the following questions: (1) How does the ratio of ET components vary across different biomes at system scale? (2) What is the impact of including or excluding EI on estimates of ET partitioning? (3) How do the factors, such as annual precipitation and LAI, influence the results of T/ET?

## 2. Materials and methods

### 2.1. Model description

#### 2.1.1. PT-JPL model

The Priestley-Taylor (PT) (Priestley and Taylor, 1972) equation has been used to estimate the potential ET from wet surfaces by replacing the aerodynamic and surface resistance terms with an empirical multiplier $\alpha$ (Zhang et al., 2009). The Priestly-Taylor Jet Propulsion Laboratory (PT-JPL) model, proposed by Fisher et al. (2008), uses some biophysical constraints to downscale the PT equation to calculate monthly actual ET. One of the essential hypotheses of the model is that plants optimize their capacity to obtain energy in parallel with the physiological capacity for transpiration (Houborg et al., 2009). The model is expressed by the following equations:

$$ET = T + EI + ES \tag{1}$$

$$T = (1-f_{wet}) f_g f_T f_M * \alpha \frac{\Delta}{\Delta + \gamma} * R_{nc} \tag{2}$$

$$EI = f_{wet} * \alpha \frac{\Delta}{\Delta + \gamma} * R_{nc} \tag{3}$$

$$ES = (f_{wet} + f_{sm}(1-f_{wet}))* \alpha \frac{\Delta}{\Delta + \gamma} * (R_{ns}-G) \tag{4}$$

$$R_{nc} = R_n - R_{ns} \tag{5}$$

$$R_{ns} = R_n * \exp(-0.61 * LAI) \tag{6}$$

where $R_n$ is net radiation (W/m$^2$), $R_{nc}$ is the net radiation for canopy (W/m$^2$), $R_{ns}$ is the net radiation to the soil (W/m$^2$), $G$ is soil heat flux (W/m$^2$), $LAI$ is leaf area index, $\Delta$ is the slope of the saturation-to-vapor pressure curve (Pa/K), $\gamma$ is the psychrometric constant ( ~ 0.066 kPa/C), and $\alpha$ is an empirical multiplier constant (1.26) (Priestley and Taylor, 1972). The other parameters restrict potential evaporation to the actual values and are described in Table 1. The PT-JPL model has been widely applied to assess ET because of its structure and excellent performance when compared to other ET models based on remote sensing (Ershadi et al., 2014; Michel et al., 2016; McCabe et al., 2016). Nevertheless, because the PT-JPL model combines many ecophysiological parameters, its performance across different biomes could be improved using optimized parameters, particularly in arid regions where ET predictions are most challenging (Garcia et al., 2013; Zhang et al., 2017).

#### 2.1.2. Parameter optimization

Initially, we identified a series of sensitive parameter sets using the

**Table 1**
Variable descriptions[a] and equations in the PT-JPL model.

| Variable | Description | Equation |
|---|---|---|
| $f_{wet}$ | Relative surface wetness | $RH^4$ |
| $f_g$ | Green canopy fraction | $f_{APAR}/f_{IPAR}$ |
| $f_T$ | Plant temperature constraint | exp [(–($T_a$–$T_{opt}$)/$T_{opt}$)$^2$] |
| $f_M$ | Plant moisture constraint | $f_{APAR}/f_{APARmax}$ |
| $f_{SM}$ | Soil moisture constraint | $RH^{(VPD/\beta)}$ |
| $f_{APAR}$ | Fraction of PAR absorbed by green vegetation cover | $m_1 EVI + b_1$ |
| $f_{IPAR}$ | Fraction of PAR intercepted by total vegetation cover | $m_2 NDVI + b_2$ |
| $f_c$ | Fractional total vegetation cover | $= f_{IPAR} = m_2 \mathrm{NDVI} + b_2$ |

[a] $RH$ is relative humidity (%), $Ta$ is mean air temperature (°C), $Topt$ is the optimum temperature for plant growth (°C), $f_{APARmax}$ is the maximum $f_{APAR}$, $VPD$ is the saturation vapor pressure deficit (kPa), $\beta$ is the sensitivity for soil moisture constraint to $VPD$ (kPa), $PRA$ is photosynthesis active radiation, $NDVI$ is the normalized difference vegetation index, $EVI$ is the enhanced vegetation index and $m_1$, $b_1$, $m_2$, and $b_2$ are parameters.

global sensitivity analysis method (Sobol', 1990, 2001; Zhang et al., 2013) and found that three parameters ($m_1$, $T_{opt}$, and $\beta$) were most sensitive to the model across different biomes. These parameters exist in different components of ET: $m_1$ is a pivotal part of the canopy constraint factor ($f_g$) and $T_{opt}$ is the optimum growth temperature of plants which controls the air temperature constraint ($f_T$); both regulate canopy transpiration. The $\beta$ parameter influences the estimation of soil evaporation. By identifying these sensitive parameters, we further optimized the parameters and improved the accuracy of the model.

We then used Bayesian optimization with the method to sample the posterior distribution for global optimization in real parameter spaces (Ter Braak, 2006). This method has been shown successful in reducing prior uncertainties of the sensitive parameters and in improving the accuracy of the model across different biomes. The detailed algorithm process can be found in Zhang et al. (2017). Five statistical measures are used to evaluate model performance in this paper, including the coefficient of determination ($R^2$), bias, relative error (RE), root-mean-square error (RMSE), and the Nash–Sutcliffe efficiency coefficient (NSE). $R^2$ ranges between 0 and 1, with higher values indicating a good simulation result; the NSE values range from $-\infty$ to 1, with NSE = 1 being the optimal value (Moriasi et al., 2007). The calculation of the statistical measures can be found in Zhu et al. (2016). We also calculate the systematic mean squared errors (RMSEs) and random mean squared errors (RMSEu) of the original and optimized model simulations following Willmott (1982).

### 2.2. Data used

#### 2.2.1. Eddy covariance data

FLUXNET (https://fluxnet.fluxdata.org/) data provide a continuous, high-quality dataset of surface heat fluxes and meteorological data across an extensive range of ecosystems (Baldocchi et al., 2001; Agarwal et al., 2010). Following the International Geosphere–Biosphere Programme (IGBP) classification (Fig. 1), we selected 75 eddy covariance towers from the FLUXNET2015 dataset across a wide range of biomes, including grasslands (GRA; 12 sites), croplands (CRO; 11 sites), evergreen needleleaf forests (ENF; 15 sites), deciduous broadleaf forests (DBF; 11 sites), evergreen broadleaf forests (EBF; 8 sites), open shrublands (OSH; 4 sites), closed shrublands (CSH; 1 site), permament wetlands (WET; 1 site), mixed forests (MF; 5 sites), savannas (SAV; 3 sites), and woody savannas (WAS; 4 sites). Our analysis was based on 616 site-years of eddy covariance data, with the data coverage at each site ranging from at least 2 years to 14 years. The observations span the period from 2001 to 2014. A general description of the 75 sites is given in Supplemental Table S1.The inputs to the PT-JPL model are monthly values aggregated from half-hourly or hourly data from the towers, including surface net radiation ($R_n$, W/m$^2$), soil heat flux (G, W/m$^2$), relative humidity (RH), air temperature ($T_a$, ˚K), and vapor pressure ($e$, Pa). We used monthly sums of sensible heat flux (H, W/m$^2$) and latent heat flux (LE, W/m$^2$) to optimize parameters in the model. The issue of non-closure of the energy balance from eddy covariance data remains largely unexplained and the best way to correct the data is still under discussion (Massman and Lee, 2002; Barr et al., 2006; Hendricks Franssen et al., 2010; Ershadi et al., 2014). The corrected fluxes of LE from FLUXNET2015 Dataset, which boosted by the closure ratio Rn-G /H + LE were used to optimize the model parameters in this study.

#### 2.2.2. Remote sensing data

We acquired the time series of the enhanced vegetation index (EVI) and the NDVI, that are required for the model inputs, from moderate-resolution imaging spectroradiometer (MODIS) products (MOD13Q1) that provide 250 m spatial and 16 day temporal resolution. We used an average of four surrounding pixels around the eddy covariance flux sites to acquire the EVI and NDVI values. The LAI, a potential factor influencing ET segmentation, was extracted from MOD15 A2 at 1 km spatial and 16 day temporal resolution. We used linear interpolation to fill the 16-day gaps between successive EVI, NDVI, and LAI records, and then integrated the satellite data into a monthly scale.

## 3. Results

### 3.1. Parameter optimization results

The optimized values of three sensitive parameters ($m_1$, $T_{opt}$, and $\beta$) and the summary of statistical performance of the original and optimized model over different biomes are shown in Supplement Table S2. In general, after using the optimized parameters, the model performed better, with lower bias and RMSE. The accuracy of the model was improved with $R^2$ values ranging from 0.43 to 0.99 and greater NSE values. The multi-year averages of (T + EI)/ET for the 75 sites, before and after the optimization of model parameters, are shown in Supplemental Fig. S1 and Table S2. Because of the different time spans, there were

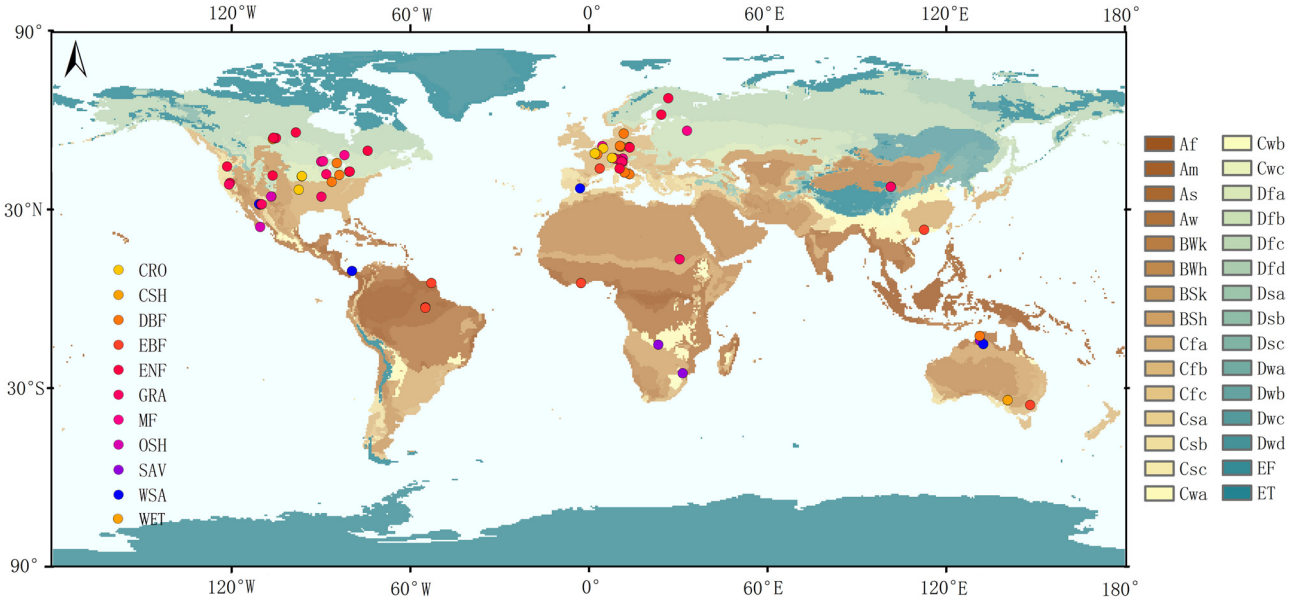


**Fig. 1.** Spatially distributed tower locations of the 75 eddy covariance flux sites used in this study. The base map is world map of Köppen-Geiger Climate Classification (http://koeppen-geiger.vu-wien.ac.at/).

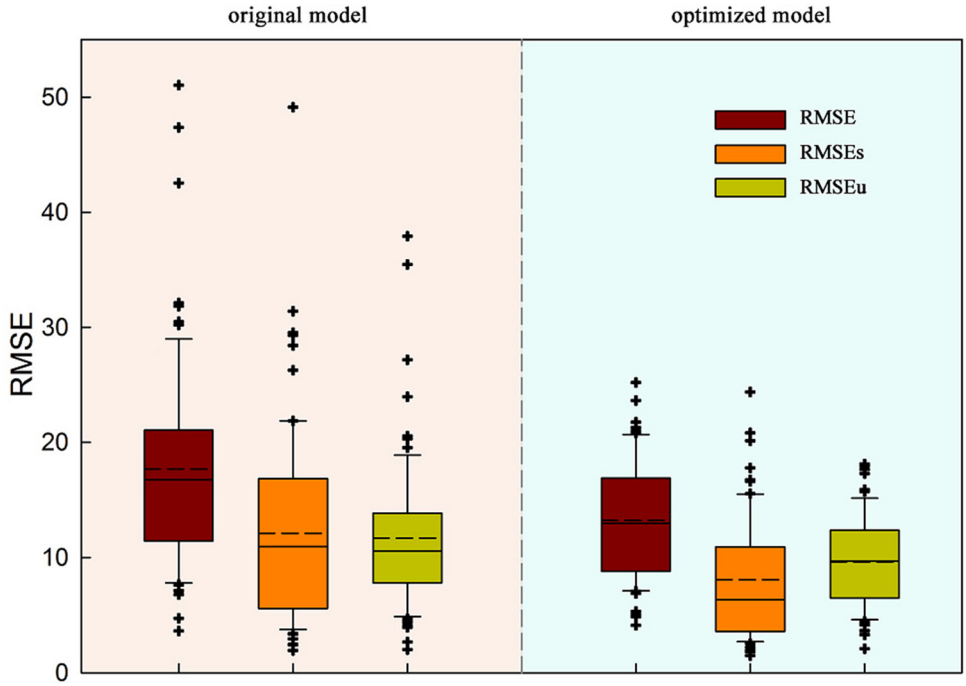


**Fig. 2.** The RMSE values, the systematic mean squared errors (RMSEs) and random mean squared errors (RMSEu) of the original and optimized model simulations cross 75 sites.

obvious differences in the (T + EI)/ET values across different sites. After optimization of the parameters, the multi-year averages of (T + EI)/ET increased at 65 sites, indicating that the proportion of soil evaporation decreased after parameter optimization for most sites. We found after parameter optimization, all of RMSE, RMSEs, RMSEu were reduced, in particular, the decrease of RMSEs is the most obvious (Fig. 2). This indicate that after parameters optimization the systematic error of the model have been reduced effectively (Willmott, 1982).

### 3.2. Canopy interception evaporation ratio

The ratios of canopy interception evaporation to precipitation (EI/P) across the 11 biomes are shown in Fig. 3. The EI/P values of the biomes were quite different, with the averages for each biome ranging from 0.05 to 0.17, but most individual values were below 0.30. The average EI/P for the EBF biome was higher than other biomes and the CSH biome had the lowest value; this may be related to different LAIs across biomes. The EI/P variation in the ENF biome was larger than other biomes, with values ranging from 0.01 to 0.34 and an average across the 15 ENF sites of 0.12. The variation may be related to different precipitation types, as the proportion of EI to precipitation increases in boreal forests where more snow is intercepted. The EI/P variation in the OSH biome was also large, ranging from 0.01 to 0.26, with an average of 0.11 among four sites. The lowest variation in EI/P occurred in the CSH biome. The range of EI/P across different biomes in our study seems within the scope of previous studies. As shown in Fig.4., we noted an increasing trend in precipitation and EI/P, and LAI and EI/P from multiple sites across different ecological types (Fig. 4A and B), though the trend was not significant. Several authors have analyzed canopy interception evaporation with results that vary significantly; only a small number of these studies were on annual timescale. Llorens and Domingo (2007) reviewed vegetation rainfall partitioning under Mediterranean climate conditions. For annual rainfall of 90–800 mm, the mean relative interception was approximately 18% for trees and 31.6% for shrubs. Miralles et al. (2010) reviewed 42 studies from different periods and found average EI/P values for the EBF biome of 0.13 with ranges from 0.08 to 0.29, the DBF biome averaged 0.19 with ranges from 0.07 to 0.27, and the ENF biome averaged 0.22 with ranges from 0.16 to 0.42.

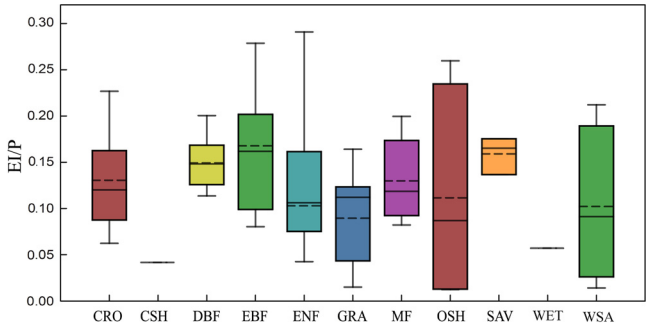


**Fig. 3.** Ratio of canopy interception evaporation to precipitation (EI/P) varies across different biomes. Boxes mark the 75th and 25th percentiles and the dashed and solid lines in the boxes refer to the average and median values, respectively.

### 3.3. Transpiration fraction

The transpiration to evapotranspiration ratios across different biomes are shown in Fig. 5A. Average T/ET values across biomes range from 0.39 (CRO biome) to 0.61 (WET biome). Large variations were noted within each biome, with the WAS biome having greatest range (0.05–0.17), followed by the EBF and ENF biomes (ranges of 0.15–0.61 and 0.3–0.79, respectively).

Previous research rarely considered vegetation interception evaporation in evapotranspiration partitions at site scale. For this study we analyzed (T + EI)/ET which can be regarded as the total contribution of vegetation to evapotranspiration. The ratios of (T + EI)/ET across the 11 biomes are shown in Fig. 5B. Average values across the different biomes ranged from 0.57 to 0.8 with the highest average in the DBF biome and the lowest in the OSH biome. The variations in the ranges of T/ET and (T + EI)/ET were significantly different, with the variation in (T + EI)/ET being smaller. After including vegetation interception

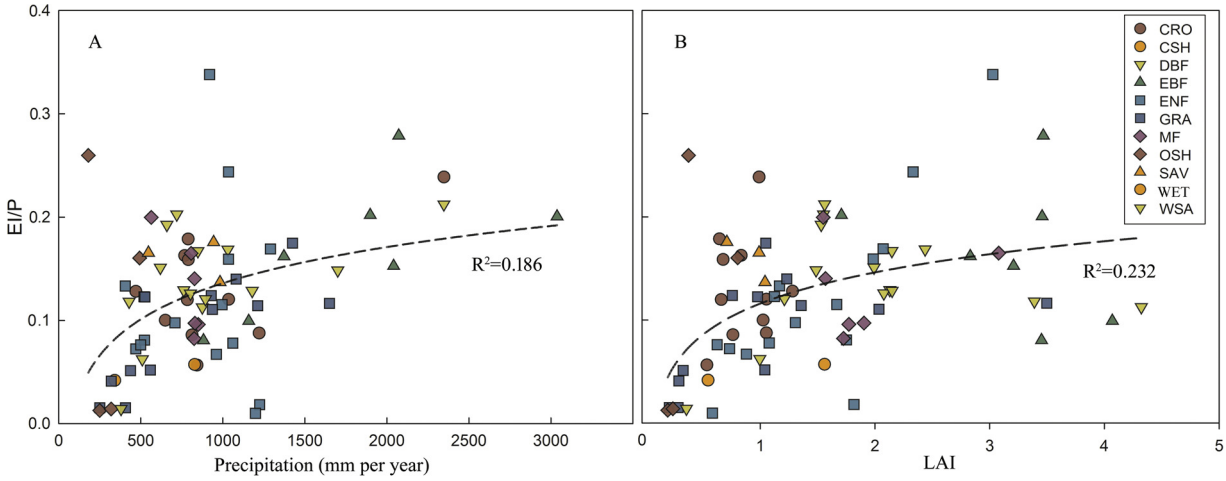


**Fig. 4.** Relationship between annual EI/P and mean annual precipitation (A), annual EI/P and mean annual LAI (B). Dashed line is the regression line, $R^2$ is the correlation coefficient.

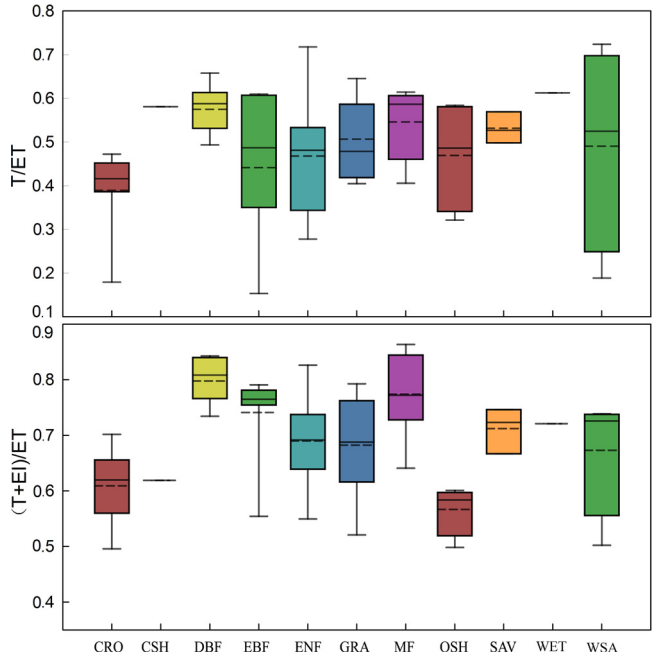


**Fig. 5.** T/ET (A) and (T + EI)/ET (B) across different biomes. Boxes mark the 75th and 25th percentiles and dashed and solid lines in the boxes refer to the average and median values, respectively.

evaporation, the largest change appeared in EBF with an average value of 0.44 for T/ET and 0.74 for (T + EI)/ET, an increase of 30%. This increase is mainly because evergreen broadleaf forests are always distributed in humid climates zone that have higher wet canopy evaporation rates than other biomes, this extrapolation is consistent with the conclusion of Wei et al. (2017). Our estimated T/ET values were much lower than the 0.80–0.90 global values that Jasechko et al. (2013) found using isotope approaches. Nevertheless, our estimated T/ET values were still within the range of previously reported values. For example, our estimated annual T/ET values, which ranged from 0.49 to 0.68 for the DBF biome were within the reported value of 0.67 ± 0.14 from Schlesinger and Jasechko (2014). The difference between our results and reported results was not large for the ENF biome (0.27–0.79 vs. 0.55 ± 0.15). We examined the statistical relationships between T/ET, (T + EI)/ET, and annual precipitation and LAI. T/ET values were found to have a negative correlation with annual precipitation (R2 = 0.205, Fig. 6A), while the relationship between T/ET and LAI was insignificantly correlated (R2 = 0.003, Fig. 6B). On the contrary, (T + EI)/ET showed an insignificantly increasing trend with increasing precipitation (R2 = 0.119; Fig. 6C), and the highest value was found at the sites with annual precipitation between 500 and 1000 mm. Notably, the relationship between (T + EI)/ET and annual LAI can be described as exponential with R2 = 0.455 (Fig. 6D).

## 4. Discussion

We compared simulation results of EI/P and T/ET with previous studies. The comparison of our T/ET results to the other site scale studies as well as some global studies is shown in Fig. 7. The range of average EI/P (0.02–0.29) and T/ET (0.29–0.72) that we found across different biomes is nearly within the scope of previous studies (Llorens and Domingo, 2007; Miralles et al., 2010; Schlesinger and Jasechko, 2014). However, the average of T/ET value were a little bit lower than previous findings, although there was a large overlap in values, which may be due to the reasons as follows. Most of the previous studies based on sites observation ignore the evaporation of precipitation intercepted by vegetation canopy, and the results of T/ET would be higher if soil evaporation and vegetation transpiration were observed separately only. Seasonal T/ET can be extremely variable within a given year at the same site because of climate change and differential plant responses (Knapp and Smith, 2001; Scott et al., 2006). Several of the previous field studies incorporated only the growing season and the average of T/ET on an annual basis, which may underestimate the transpiration fraction (Sutanto et al., 2014). Different techniques and research scales may also contribute to the variability, for instance the isotope-based approach constrained by hydrologic decoupling always overestimates T/ET (Jasechko et al., 2013).

This study provides a method for ET partitioning at the ecosystem scale with results that reflect the characteristics across different biomes. The T/ET fraction has been shown to change among ecosystems based on the type of vegetation, different soil infiltration, and climatic conditions, as well as water table depth, including lateral groundwater flow (Kurc and Small, 2007; Moran et al., 2009; Cavanaugh et al., 2011; Raz-Yaseef et al., 2012; Maxwell and Condon,2016). As we know, for a specific vegetation type, T/ET generally increase as vegetation cover increases (Ashktorab et al., 1994; Young et al., 2009; Raz-Yaseef et al., 2010a; Wang et al., 2010; Fatichi and Pappas, 2017). However, in this study we observed that T/ET varies largely across all LAI ranges over different biomes and the correlation between them is insignificant (Fig. 6B). This is mainly because of this study is focused on annual time scales and the obvious temporal variation of T/ET has been identified within a year (Sutanto et al., 2014). These findings are consistent with

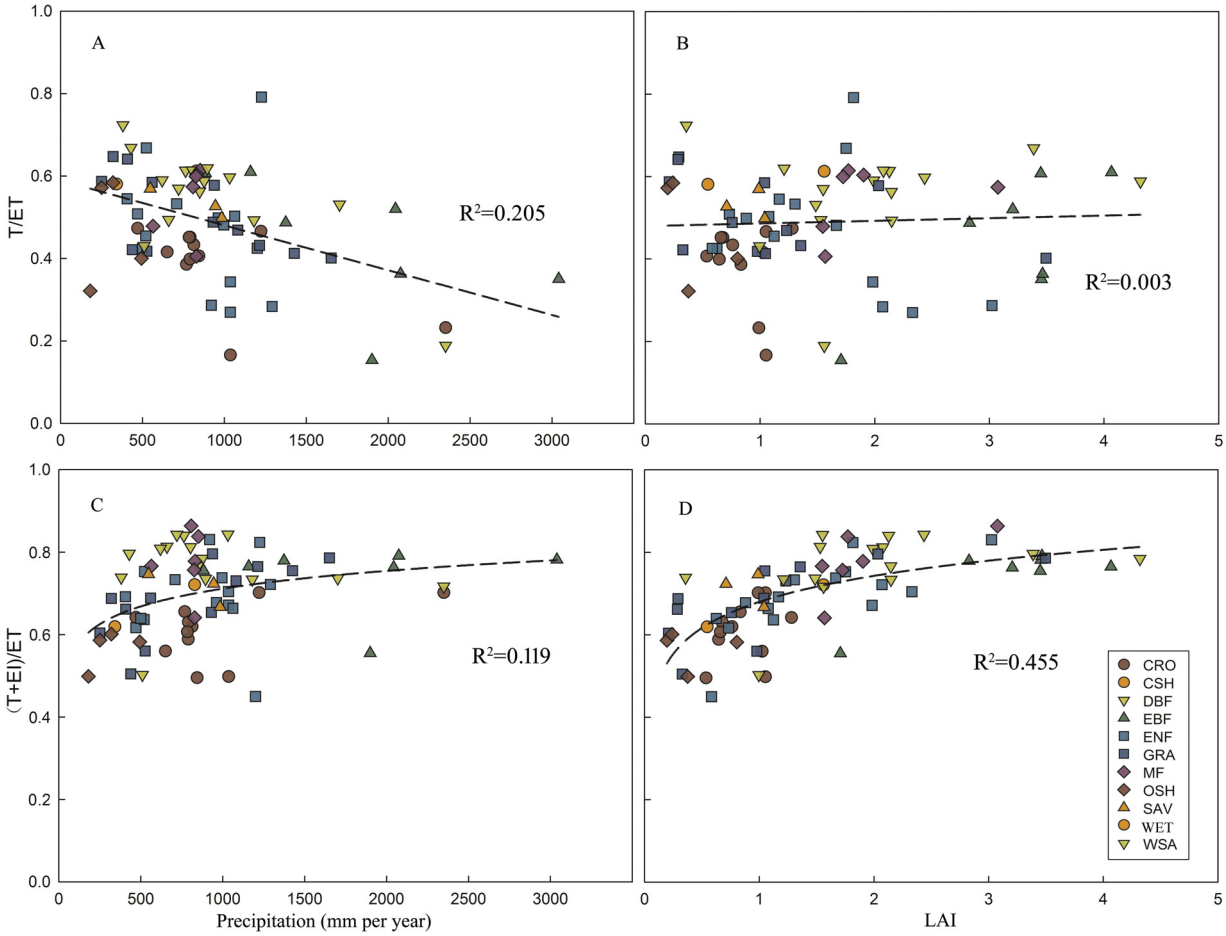


**Fig. 6.** General relationship between (A) mean annual precipitation and annual T/ET; (B) mean annual leaf area index (LAI) and annual T/ET; (C) mean annual precipitation and annual (T + EI)/ET; (D) mean annual leaf area index (LAI) and annual (T + EI)/ET in simulation results. Each point corresponds to the multi-year average value for the site. Dashed line is the regression line, $R^2$ is the correlation coefficient.

the study by Wang et al. (2014), which synthesized published research for both agricultural and natural data subsets. Thus, the control on T/ET under a fixed LAI across different biomes is different from that over a specific vegetation type, and it is difficult to properly partition global ET solely based on information of LAI. Nevertheless, our results supported a similar exponential relationship between annual (T + EI)/ET and LAI demonstrating that (T + EI)/ET increases with increases in LAI (Fig. 6D). This indicates that with increasing vegetation coverage, the

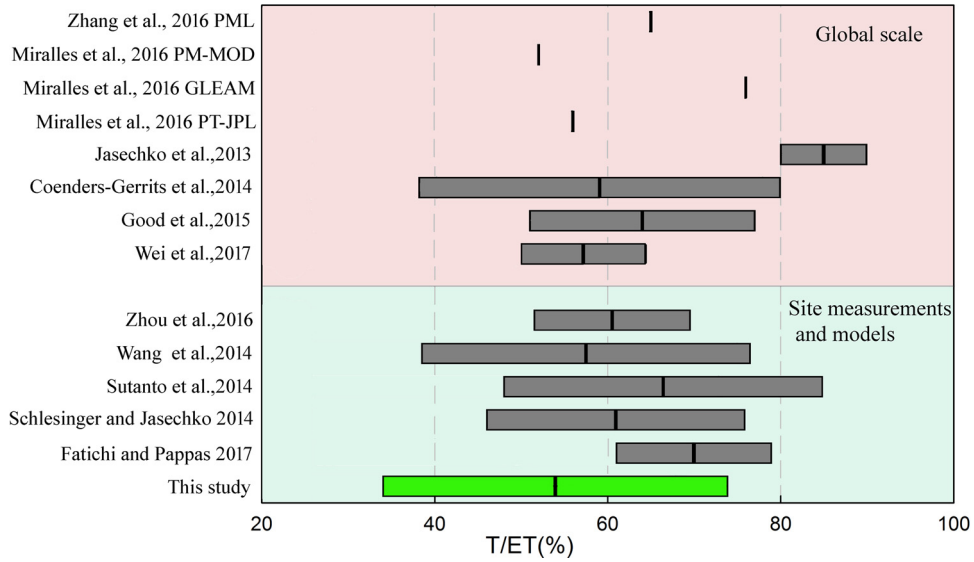


**Fig. 7.** Comparison of T/ET estimated by different methods from global and site scale. The rectangle represents the standard deviation or the reported ranges in the published literature.

total contribution of vegetation to evapotranspiration, including transpiration and canopy interception evaporation increases.

Previous research mainly focused on studying the relationship between T/ET and growing-season precipitation amount or precipitation patterns. The results indicated that T/ET generally decreases with total growing-season precipitation (Reynolds et al., 2000; Loik et al., 2004; Moran et al., 2009). However, Schlesinger and Jasechko (2014) compiled 81 studies that partitioned ET into transpiration and evaporation, including experimental observations and simulation results, and found a weak correlation between T/ET and precipitation. In our study the regression between T/ET and precipitation shows a demonstrable decrease in T/ET across all sites with increasing annual precipitation ($R^2$ = 0.205, Fig. 6A), but the (T + EI)/ET showed an increasing trend with increasing precipitation ($R^2$ = 0.119; Fig. 6C). We can speculate the reason for a weak correlation between T/ET and annual precipitation in the research of Schlesinger and Jasechko (2014) is that the 81 previous studies did not consider the interception evaporation of vegetation, and mixed T and EI creates uncertainty of the relationship.

We compared ET and its three components with LAI and annual precipitation to further analyze the relationships. Scatter plots between LAI, annual precipitation, and T, EI, ES, and ET are shown in Supplemental Figs. S2 and S3. We found that T, EI, and ET increase with increasing LAI, but ES showed negative correlation with LAI. The relationships between precipitation and the components of evapotranspiration varied. All the values of T, EI, ES, and ET showed increasing trends with increasing precipitation, however, the slope of the trends were different. The correlation of EI to P was the most obvious, followed by that of ES to P. The correlation of *T* with increasing P showed the weakest correlation. The different trends among T, EI, ES and P most likely lead to the ratio of T/ET decreasing with increasing precipitation.

We also selected some results of experimental observations from previous studies that we deemed reliable to contrast the relationship between T/ET and annual precipitation (Fig. 8). We excluded results only estimated from biophysical models, focusing on 21 studies that used eddy covariance, sap-flow measurements, isotopic approaches, or these approaches coupled with models (Supplemental Table S3). Fig. 8 shows that the range of T/ET by model simulation results in this study is close to previous researches. From this study, T/ET show negative correlation with annual precipitation ($R^2$ = 0.205). However, there is no relationship of T/ET versus precipitation from the 21 previous studies ($R^2$ = 0.014). The discrepancy of the relationship may be due to the water flux partitioning with or without incorporating the EI term. The sites with annual precipitation less than 250 mm is not sufficient in our research, however, previous study has shown that the water vapor

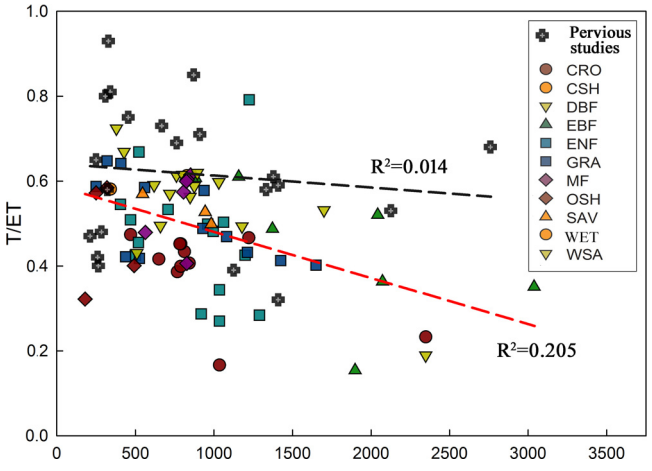


**Fig. 8.** Relationship between T/ET to annual precipitation. The cross points represent results of experimental observations from previous studies. Dashed line is the regression line between annual precipitation and T/ET.

interaction in the desert is more complex (Li et al.,2016).Our study used an optimized satellite-based ET model to partition evapotranspiration into three components T, EI, ES. Although we made efforts to improve the accuracy of the results by using forced energy closure and optimizing sensitivity parameters, many uncertainties still affecting the ET partition results remain. The random uncertainty in the measured variable as forcing data estimated at half-hourly resolution and aggregated to monthly scale and the impacts of inherent observation error on model simulation play vital functions. The correction method of the unclosed energy problem and spatial resolution mismatch between flux tower sites and NDVI, EVI, and LAI derived from satellite data also influences the accuracy of the estimation (Ershadi et al., 2013). Other than the three most sensitive parameters, other empirical parameters in the algorithm structure may lead to large uncertainties in the results (Feng et al., 2015). After the parameters have been optimized by the DE-MC method, the principal source of model error was attributable to structure and inherent assumptions of the model (Zhu et al., 2014).

## 5. Conclusions

Based on the parameter-optimized PT-JPL model, we used monthly flux tower measurements from 75 sites across 11 different biomes (taken over multiple years) to simulate ET, and realized generally satisfactory results. We calculated three components of evapotranspiration and analyzed relationships between ET partitioning and potential influencing factors. Our findings indicate obvious differences in the evapotranspiration partitions across different biomes as well as variations among sites within the same biome. The T/ET values ranged from 0.39 to 0.59 across biomes, but the (T + EI)/ET ratio was limited to a relatively narrow band from 0.57 to 0.8. The results highlight the importance of vegetation interception evaporation. With and without incorporating the EI term may affect prior discrepancies in water flux partitioning. Therefore, it should be prudent to compare the observation ET partition results excluding EI generally with model results. Meanwhile, There are significant distinction between the relationship of annual precipitation, LAI and T/ET, (T + EI)/ET. The T/ET showed an obvious decreasing trend with increasing annual precipitation ($R^2$ = 0.205), but there was no significant correlation between T/ET and LAI ($R^2$ = 0.003). The exponential relationship between (T + EI)/ET and annual LAI was generally obvious ($R^2$ = 0.455), but the relationship between (T + EI) /ET and annual precipitation was not significant ($R^2$ = 0.119).

Our method provides a reference and guidance for future estimates of ET partitioning studies that can be easily applied to longer time scales. A continuously estimated T/ET ratio can be used to monitor ecosystem dynamic responses to climatic change. Nevertheless, some uncertainties exist in the results of ET segmentation and further validation of the model results is required. Additionally, sites with low annual precipitation (less than 250 mm) were under-represented in our study and the characteristics of ET partitions are not obvious.

## Acknowledgments

Funding: This research was supported by the National Key R&D Program of China (2016YFC0500203) and National Natural Science Foundation of China (nos. 31370467 and 41571016).

This project used eddy covariance data from the FLUXNET2015 Dataset acquired and shared by the FLUXNET community, including these networks: AmeriFlux, AfriFlux, AsiaFlux, CarboAfrica, CarboEuropeIP, CarboItaly, CarboMont, ChinaFlux, Fluxnet-Canada, GreenGrass, ICOS, KoFlux, LBA, NECC, OzFlux-TERN, TCOS-Siberia, and USCCC. The ERA-Interim reanalysis data are provided by ECMWF and processed by LSCE. The FLUXNET eddy covariance data processing and harmonization was carried out by the European Fluxes Database Cluster, AmeriFlux Management Project, and Fluxdata project of FLUXNET, with the support of CDIAC and ICOS Ecosystem Thematic

Center, and the OzFlux, ChinaFlux and AsiaFlux offices. MODIS NDVI, EVI, LAI satellite products were obtained online (https://modis.ornl.gov/).

## Appendix A. Supplementary data

Supplementary material related to this article can be found, in the online version, at doi:https://doi.org/10.1016/j.agrformet.2018.05.023.

## References


Agarwal, D.A., Humphrey, M., Beekwilder, N.F., Jackson, K.R., Goode, M.M., van Ingen, C., 2010. A data-centered collaboration portal to support global carbon-flux analysis. Concurr. Comput. Pract. Exp. 22 (17), 2323–2334. http://dx.doi.org/10.1002/cpe.1600.

Ashktorab, H., Pruitt, W.O., Member, ASCE, Paw U, K.T., 1994. Partitioning of evapotranspiration using lysimeter and micro-Bowen-ratio system. J. Irrig. Drain. Eng. 120, 450–464. http://dx.doi.org/10.1061/(ASCE)0733-9437(1994)120:2(450).

Baldocchi, D., Falge, E., Gu, L., Olson, R., Hollinger, D., Running, S., Anthoni, P., Bernhofer, C., Davis, K., Evans, R., et al., 2001. FLUXNET: a new tool to study the temporal and spatial variability of ecosystem-scale carbon dioxide, water vapor, and energy flux densities. Bull. Am. Meteorol. Soc. 82, 2415–2434. http://dx.doi.org/10.1175/1520-0477(2001)082<2415:FANTTS>2.3.CO;2.

Barbour, M.M., Hunt, J.E., Walcroft, A.S., Rogers, G.N.D., McSeveny, T.M., Whitehead, D., 2005. Components of ecosystem evaporation in a temperate coniferous rainforest, with canopy transpiration scaled using sap-wood density. N. Phytol. 165, 549–558. http://dx.doi.org/10.1111/j.1469-8137.2004.01257.x.

Barr, A.G., Morgenstern, K., Black, T.A., McCaughey, J.H., Nesic, Z., 2006. Surface energy balance closure by the eddy-covariance method above three boreal forest stands and implications for the measurement of the $CO_2$ flux. Agric. For. Meteorol. 140 (1–4), 322–337. http://dx.doi.org/10.1016/j.agrformet.2006.08.007.

Blyth, E., Harding, R.J., 2011. Methods to separate observed global evapotranspiration into the interception, transpiration and soil surface evaporation components. Hydrol. Process. 25, 4063–4068. http://dx.doi.org/10.1002/hyp.8409.

Cavanaugh, M.L., Kurc, S.A., Scott, R.L., 2011. Evapotranspiration partitioning in semiarid shrubland ecosystem: a two-site evaluation of soil moisture control on transpiration. Ecohydrology 4, 671–681. http://dx.doi.org/10.1002/eco.157.

Choudhury, B.J., DiGirolamo, N.E., 1998. A biophysical process-based estimate of global land surface evaporation using satellite and ancillary data; I. Model description and comparison with observations. J. Hydrol. 205, 164–185. http://dx.doi.org/10.1016/S0022-1694(97)00147-9.

Cleugh, H.A., Leuning, R., Mu, Q.Z., Running, S.W., 2007. Regional evaporation estimates from flux tower and MODIS satellite data. Remote Sens. Environ. 106 (3), 285–304. http://dx.doi.org/10.1016/j.rse.2006.07.007.

Coenders-Gerrits, A.M.J., van der Ent, R.J., Bogaard, T.A., Wang-Erlandsson, L., Hrachowitz, M., Savenije, H.H.G., 2014. Uncertainties in transpiration estimates. Nature 506, E1–E2. http://dx.doi.org/10.1038/nature12925.

Dirmeyer, P.A., Gao, X., Zha, M., Guo, Z., Oki, T., Hanasaki, N., 2006. GSWP-2: multimodel analysis and implications for our perception of the land surface. Bull. Am. Meteorol. Soc. 87, 1381–1397. http://dx.doi.org/10.1175/BAMS-87-10-1381.

Ershadi, A., McCabe, M.F., Evans, J.P., Walker, J.P., 2013. Effects of spatial aggregation on the multi-scale estimation of evapotranspiration. Remote Sens. Environ. 131, 51–62. http://dx.doi.org/10.1016/j.rse.2012.12.007.

Ershadi, A., McCabe, M.F., Evans, J.P., Chaney, N.W., Wood, E.F., 2014. Multi-site evaluation of terrestrial evaporation models using FLUXNET data. Agric. For. Meteorol. 187, 46–61. http://dx.doi.org/10.1016/j.agrformet.2013.11.008.

Fatichi, S., Pappas, C., 2017. Constrained variability of modeled T: ET ratio across biomes. Geophys. Res. Lett. 44, 6795–6803. http://dx.doi.org/10.1002/2017GL074041.

Feng, F., Chen, J.Q., Li, X.L., Yao, Y.J., Liang, S.L., Liu, M., Zhang, N.N., Guo, Y., Yu, J., Sun, M.M., 2015. Validity of five satellite-based latent heat flux algorithms for semiarid ecosystems. Remote Sens. 7 (12), 16733–16755. http://dx.doi.org/10.3390/rs71215853.

Ferretti, D.F., Pendall, E., Morgan, J.A., Nelson, J.A., LeCain, D., Mosier, A.R., 2003. Partitioning evapotranspiration fluxes from a Colorado grassland using stable isotopes: seasonal variations and ecosystem implications of elevated atmospheric $CO_2$. Plant Soil 254, 291–303. http://dx.doi.org/10.1023/A:1025511618571.

Ffolliott, P.F., Gottfried, G.J., Cohen, Y., Schiller, G., 2003. Transpiration by dryland oaks: studies in the south-western United States and northern Israel. J. Arid Environ. 55, 595–605. http://dx.doi.org/10.1016/S0140-1963(02)00290-2.

Fisher, J.B., Tu, K.P., Baldocchi, D.D., 2008. Global estimates of the land-atmosphere water flux based on monthly AVHRR and ISLSCP-II data, validated at 16 FLUXNET sites. Remote Sens. Environ. 112 (3), 901–919. http://dx.doi.org/10.1016/j.rse.2007.06.025.

Fisher, J.B., et al., 2017. The future of evapotranspiration: global requirements for ecosystem functioning, carbon and climate feedbacks, agricultural management, and water resources. Water Resour. Res. 53, 2618–2626. http://dx.doi.org/10.1002/2016WR020175.

Garcia, M., Sandholt, I., Ceccato, P., Ridler, M., Mougin, E., Kergoat, L., Morillas, L., Timouk, F., Fensholt, R., Domingo, F., 2013. Actual evapotranspiration in drylands derived from in-situ and satellite data: assessing biophysical constraints. Remote Sens. Environ. 131, 103–118. http://dx.doi.org/10.1016/j.rse.2012.12.016.

Hendricks Franssen, H.J., Stöckli, R., Lehner, I., Rotenberg, E., Seneviratne, S.I., 2010. Energy balance closure of eddy-covariance data: a multisite analysis for European FLUXNET stations. Agric. For. Meteorol. 150 (12), 1553–1567. http://dx.doi.org/10.1016/j.agrformet.2010.08.005.

Herbst, M., Kappen, L., Thamm, F., Vanselow, R., 1996. Simultaneous measurements of transpiration, soil evaporation and total evaporation in a maize field in northern Germany. J. Exp. Bot. 47, 1957–1962. http://dx.doi.org/10.1093/jxb/47.12.1957.

Houborg, R., Anderson, M.C., Norman, J.M., Wilson, T., Meyers, T., 2009. Intercomparison of a 'bottom-up' and 'top-down' modeling paradigm for estimating carbon and energy fluxes over a variety of vegetative regimes across the U.S. Agric. For. Meteorol. 149 (11), 1875–1895. http://dx.doi.org/10.1016/j.agrformet.2009.06.014.

Jasechko, S., Sharp, Z.D., Gibson, J.J., Birks, S.J., Yi, Y., Fawcett, P.J., 2013. Terrestrial water fluxes dominated by transpiration. Nature 496, 347–350. http://dx.doi.org/10.1038/nature11983.

Knapp, A.K., Smith, M.D., 2001. Variation among biomes in temporal dynamics of aboveground primary production. Science 291, 481–484. http://dx.doi.org/10.1126/science.291.5503.481.

Kool, D., Agam, N., Lazarovitch, N., Heitman, J.L., Sauer, T.J., Ben-Gal, A., 2014. A review of approaches for evapotranspiration partitioning. Agric. For. Meteorol. 184, 56–70.

Kurc, S.A., Small, E.E., 2007. Soil moisture variations and ecosystem-scale fluxes of water and carbon in semiarid grassland and shrubland. Water Resour. Res. 43, 1–15. http://dx.doi.org/10.1016/j.agrformet.2013.09.003.

Lawrence, D.M., Thornton, P.E., Oleson, K.W., Bonan, G.B., 2007. The partitioning of evapotranspiration into transpiration, soil evaporation, and canopy interception in a GCM: impacts on land–atmosphere interaction. J. Hydrometeorol. 8, 862–880. http://dx.doi.org/10.1175/JHM596.1.

Li, X., Yang, K., Zhou, Y., 2016. Progress in the study of oasis-desert interactions. Agric. For. Meteorol. 230–231, 1–7. http://dx.doi.org/10.1016/j.agrformet.2016.08.022.

Liu, S.M., Xu, Z.W., Song, L.S., Zhao, Q.Y., Ge, Y., Xu, T.R., Ma, Y.F., Zhu, Z.L., Jia, Z.Z., Zhang, F., 2016. Upscaling evapotranspiration measurements from multi-site to the satellite pixel scale over heterogeneous land surfaces. Agric. For. Meteorol. 230–231, 97–113. http://dx.doi.org/10.1016/j.agrformet.2016.04.008.

Llorens, P., Domingo, F., 2007. Rainfall partitioning by vegetation under Mediterranean conditions. A review of studies in Europe. J. Hydrol. 335, 37–54. http://dx.doi.org/10.1016/j.jhydrol.2006.10.032.

Loik, M.E., Breshears, D.D., Lauenroth, W.K., Belnap, J., 2004. A multi-scale perspective of water pulses in dryland ecosystems: climatology and ecohydrology of the western USA. Oecologia 141, 269–281. http://dx.doi.org/10.1007/s00442-004-1570-y.

Massman, W.J., Lee, X., 2002. Eddy covariance flux corrections and uncertainties in long-term studies of carbon and energy exchanges. Agric. For. Meteorol. 113, 121–144. http://dx.doi.org/10.1016/S0168-1923(02)00105-3.

Maxwell, R.M., Condon, L.E., 2016. Connections between groundwater flow and transpiration partitioning. Science 353 (6297), 377–380. http://dx.doi.org/10.1126/science.aaf7891.

McCabe, M.F., Ershadi, A., Jimenez, C., Miralles, D.G., Michel, D., Wood, E.F., 2016. The GEWEX LandFlux project: evaluation of model evaporation using tower-based and globally gridded forcing data. Geosci. Model Dev. 9 (1), 283–305. http://dx.doi.org/10.5194/gmd-9-283-2016.

Michel, D., Jiménez, C., Miralles, D.G., Jung, M., Hirschi, M., Ershadi, A., Martens, B., McCabe, M.F., Fisher, J.B., Mu, Q., Seneviratne, S.I., Wood, E.F., Fernández-Prieto, D., 2016. The WACMOS-ET project–part 1: tower-scale evaluation of four remote-sensing-based evapotranspiration algorithms. Hydrol. Earth Syst. Sci. 20, 803–822. http://dx.doi.org/10.5194/hess-20-803-2016.

Miralles, D.G., Gash, J.H., Holmes, R.H., De Jeu, R.A.M., Dolman, A.J., 2010. Global canopy interception from satellite observations. J. Geophys. Res. 115, D16122. http://dx.doi.org/10.1029/2009JD013530.

Miralles, D.G., De Jeu, R.A.M., Gash, J.H., Holmes, T.R.H., Dolman, A.J., 2011. Magnitude and variability of land evaporation and its components at the global scale. Hydrol. Earth Syst. Sci. 15, 967–981. http://dx.doi.org/10.5194/hess-15-967-2011.

Mitchell, P.J., Veneklaas, E., Lambers, H., Burgess, S.S.O., 2009. Partitioning of evapotranspiration in a semi-arid eucalypt woodland in south-western Australia. Agric. For. Meteorol. 149, 25–37. http://dx.doi.org/10.1016/j.agrformet.2008.07.008.

Moran, M.S., Scott, R.L., Keefer, T.O., Emmerich, W.E., Hernandez, M., Nearing, G.S., Paige, G.B., Cosh, M.H., O'Neill, P.E., 2009. Partitioning evapotranspiration in semiarid grassland and shrubland ecosystems using time series of soil surface temperature. Agric. For. Meteorol. 149, 59–72. http://dx.doi.org/10.1016/j.agrformet.2008.07.004.

Moriasi, D.N., Arnold, J.G., Van Liew, M.W., Bingner, R.L., Harmel, R.D., Veith, T.L., 2007. Model evaluation guidelines for systematic quantification of accuracy in watershed simulations. Trans. ASABE 50 (3), 885–900. http://dx.doi.org/10.13031/2013.23153.

Mu, Q., Heinsch, F.A., Zhao, M., Running, S.W., 2007. Development of a global evapotranspiration algorithm based on MODIS and global meteorology data. Remote Sens. Environ. 111, 519–536. http://dx.doi.org/10.1016/j.rse.2007.04.015.

Mu, Q.Z., Zhao, M.S., Running, S.W., 2011. Improvements to a MODIS global terrestrial evapotranspiration algorithm. Remote Sens. Environ. 115 (8), 1781–1800. http://dx.doi.org/10.1016/j.rse.2011.02.019.

Muzylo, A., Llorens, P., Valente, F., Keizer, J.J., Domingo, F., Gash, J.H.C., 2009. A review of rainfall interception modelling. J. Hydrol. 370, 191–206. http://dx.doi.org/10.1016/j.jhydrol.2009.02.058.

Priestley, C.H.B., Taylor, R.J., 1972. On the assessment of surface heat flux and evaporation using large-scale parameters. Mon. Weather Rev. 100, 81–92. http://dx.doi.org/10.1175/1520-0493(1972)100<0081:OTAOSH>2.3.CO;2.

Raz-Yaseef, N., Rotenberg, E., Yakir, D., 2010a. Effects of spatial variations in soil

evaporation caused by tree shading on water flux partitioning in a semi-arid pine forest. Agric. For. Meteorol. 150, 454–462. http://dx.doi.org/10.1016/j.agrformet.2010.01.010.

Raz-Yaseef, N., Yakir, D., Schiller, G., Cohen, S., 2012. Dynamics of evapotranspiration partitioning in a semi-arid forest as affected by temporal rainfall patterns. Agric. For. Meteorol. 157, 77–85. http://dx.doi.org/10.1016/j.agrformet.2012.01.015.

Reynolds, J.F., Kemp, P.R., Tenhunen, J.D., 2000. Effects of long-term rainfall variability on evapotranspiration and soil water distribution in the Chihuahuan desert: a modeling analysis. Plant Ecol. 150, 145–159. http://dx.doi.org/10.1023/A:1026530522612.

Rothfuss, Y., Biron, P., Braud, I., Canale, L., Durant, J.-L., Gaudet, J.-P., Richard, P., Vauclin, M., Bariac, T., 2010. Partitioning evapotranspiration fluxes into soil evaporation and plant transpiration using water stable isotopes under controlled conditions. Hydrol. Process. 24, 3177–3194. http://dx.doi.org/10.1002/hyp.7743.

Roupsard, O., Bonnefond, J.-M., Irvine, M., Berbigier, P., Nouvellon, Y., Dauzat, J., Taga, S., Hamel, O., Jourdan, C., Saint-André, L., Mialet-Serra, I., Labouisse, J.-P., Epron, D., Joffre, R., Braconnier, S., Rouzière, A., Navarro, M., Boullet, J.-P., 2006. Partitioning energy and evapo-trasnpiration above and below a tropical palm canopy. Agric. For. Meteorol. 139, 252–268. http://dx.doi.org/10.1016/j.agrformet.2006.07.006.

Schlesinger, W.H., Jasechko, S., 2014. Transpiration in the global water cycle. Agric. For. Meteorol. 189–190, 115–117. http://dx.doi.org/10.1016/j.agrformet.2014.01.011.

Scott, R.L., Huxman, T.E., Cable, W.L., Emmerich, W.E., 2006. Partitioning of evapotranspiration and its relation to carbon dioxide exchange in a Chihuahuan desert shrubland. Hydrol. Process. 20, 3227–3243. http://dx.doi.org/10.1002/hyp.6329.

Seneviratne, S.I., Lüthi, D., Litschi, M., Schär, C., 2006. Land-atmosphere coupling and climate change in Europe. Nature 443, 205–209. http://dx.doi.org/10.1038/nature05095.

Sobol', I.M., 1990. On sensitivity estimation of nonlinear mathematical models. Matem. Mod. 2 (1), 112–118.

Sobol', I.M., 2001. Global sensitivity indices for nonlinear mathematical models and their Monte Carlo estimates. Math. Comput. Simul. 55 (1–3), 271–280. http://dx.doi.org/10.1016/S0378-4754(00)00270-6.

Sutanto, S.J., Wenninger, J., Coenders-Gerrits, A.M.J., Uhlenbrook, S., 2012. Partitioning of evaporation into transpiration, soil evaporation and interception: a comparison between isotope measurements and a HYDRUS-1D model. Hydrol. Earth Syst. Sci. 16, 2605–2616. http://dx.doi.org/10.5194/hess-16-2605-2012.

Sutanto, S.J., van den Hurk, B., Dirmeyer, P.A., Seneviratne, S.I., Röckmann, T., Trenberth, K.E., Blyth, E.M., Wenninger, J., Hoffmann, G., 2014. HESS opinions "A perspective on isotope versus non-isotope approaches to determine the contribution of transpiration to total evaporation". Hydrol. Earth Syst. Sci. 18, 2815–2827. http://dx.doi.org/10.5194/hess-18-2815-2014.

Ter Braak, C.J.F., 2006. A Markov Chain Monte Carlo version of the genetic algorithm differential evolution: easy Bayesian computing for real parameter spaces. Stat. Comput. 16 (3), 239–249. http://dx.doi.org/10.1007/s11222-006-8769-1.

Trenberth, K.E., Fasullo, J.T., Kiehl, J., 2009. Earth's global energy budget. Bull. Am. Meteorol. Soc. 90, 311–323. http://dx.doi.org/10.1175/2008BAMS2634.1.

Wang, L., Caylor, K.K., Villegas, J.C., Barron-Gafford, G.A., Breshears, D.D., Huxman, T.E., 2010. Partitioning evapotranspiration across gradients of woody plant cover: assessment of a stable isotope technique. Geophys. Res. Lett. 37, L09401. http://dx.doi.org/10.1029/2010GL043228.

Wang, L., Good, S.P., Caylor, K.K., Cernusak, L.A., 2012. Direct quantification of leaf transpiration isotopic composition. Agric. For. Meteorol. 154–155, 127–135. http://dx.doi.org/10.1016/j.agrformet.2011.10.018.

Wang, L., Good, S.P., Caylor, K.K., 2014. Global synthesis of vegetation control on evapotranspiration partitioning. Geophys. Res. Lett. 41, 6753–6757. http://dx.doi.org/10.1002/2014GL061439.

Wei, Z., Yoshimura, K., Wang, L., Miralles, D.G., Jasechko, S., Lee, X., 2017. Revisiting the contribution of transpiration to global terrestrial evapotranspiration. Geophys. Res. Lett. 44, 2792–2801. http://dx.doi.org/10.1002/2016GL072235.

Willmott, C.J., 1982. Some comments on the evaluation of model performance. Bull. Am. Meteorol. Soc. 63, 1309–1313.

Xu, Z., Yang, H., Liu, F., An, S., Cui, J., Wang, Z., Liu, S., 2008. Partitioning evapotranspiration flux components in a subalpine shrubland based on stable isotopic measurements. Bot. Stud. 49, 351–361.

Yakir, D., Wang, X.F., 1996. Fluxes of $CO_2$ and water between terrestrial vegetation and the atmosphere estimated from isotope measurements. Nature 380, 515–517. http://dx.doi.org/10.1038/380515a0.

Yepez, E.A., Williams, D.G., Scott, R.L., Lin, G., 2003. Partitioning overstory and understory evapotranspiration in a semi-arid savanna woodland from the isotopic composition of water vapor. Agric. For. Meteorol. 119, 53–68. http://dx.doi.org/10.1016/S0168-1923(03)00116-3.

Young, M.H., Caldwell, T.G., Meadows, D.G., Fenstermaker, L.F., 2009. Variability of soil physical and hydraulic properties at the Mojave global change facility, Nevada: implications for water budget and evapotranspiration. J. Arid Environ. 73, 733–744. http://dx.doi.org/10.1016/j.jaridenv.2009.01.015.

Zhang, K., Kimball, J.S., Mu, Q., Jones, L.A., Goetz, S.J., Running, S.W., 2009. Satellite based analysis of northern ET trends and associated changes in the regional water balance from 1983 to 2005. J. Hydrol. 379, 92–110. http://dx.doi.org/10.1016/j.jhydrol.2009.09.047.

Zhang, K., Kimball, J.S., Nemani, R.R., Running, S.W., 2010. A continuous satellite-derived global record of land surface evapotranspiration from 1983 to 2006. Water Resour. Res. 46, W09522. http://dx.doi.org/10.1029/2009WR008800.

Zhang, C., Chu, J.G., Fu, G.T., 2013. Sobol's sensitivity analysis fora distributed hydrological model of Yichun River Basin, China. J. Hydrol. 480, 58–68. http://dx.doi.org/10.1016/j.jhydrol.2012.12.005.

Zhang, K., Ma, J., Zhu, G., Ma, T., Han, T., Feng, L.L., 2017. Parameter sensitivity analysis and optimization for a satellite-based evapotranspiration model across multiple sites using moderate resolution imaging spectroradiometer and flux data. J. Geophys. Res. Atmos. 122, 230–245. http://dx.doi.org/10.1002/ 2016JD025768.

Zhu, G.F., Li, X., Su, Y.H., Zhang, K., Bai, Y., Ma, J.Z., Li, C.B., Hu, X.L., He, J.H., 2014. Simultaneously assimilating multivariate data sets into the two-source evapotranspiration model by Bayesian approach: application to spring maize in an arid region of northwestern China. Geosci. Model Dev. 7 (4), 1467–1482. http://dx.doi.org/10.5194/gmd-7-1467-2014.

Zhu, G.F., Li, X., Zhang, K., Ding, Z.Y., Han, T., Ma, J.Z., Huang, C.L., He, J.H., Ma, T., 2016. Multi-model ensemble prediction of terrestrial evapotranspiration across north China using Bayesian model averaging. Hydrol. Process. 30 (16), 2861–2879. http://dx.doi.org/10.1002/hyp.10832.